ARMY RESEARCH LABORATORY

Numerical Analysis of the Ballistic Impact of Tungsten-Based Penetrators on Hot-Pressed Boron Carbide Targets

by Constantine G. Fountzoulas and Jerry C. LaSalvia

ARL-TR-6623 **September 2013**

NOTICES

Disclaimers

The findings in this report are not to be construed as an official Department of the Army position unless so designated by other authorized documents.

Citation of manufacturer's or trade names does not constitute an official endorsement or approval of the use thereof.

Destroy this report when it is no longer needed. Do not return it to the originator.

Army Research Laboratory
Aberdeen Proving Ground, MD 21005-5069

ARL-TR-6623 **September 2013**

Numerical Analysis of the Ballistic Impact of Tungsten-Based Penetrators on Hot-Pressed Boron Carbide Targets

Constantine G. Fountzoulas and Jerry C. LaSalvia
Weapons and Materials Research Directorate, ARL

REPORT DOCUMENTATION PAGE	Form Approved OMB No. 0704-0188

1. REPORT DATE *(DD-MM-YYYY)*	2. REPORT TYPE	3. DATES COVERED (From - To)
September 2013	Final	December 2012

4. TITLE AND SUBTITLE
Numerical Analysis of the Ballistic Impact of Tungsten-Based Penetrators on Hot-Pressed Boron Carbide Targets

5a. CONTRACT NUMBER

5b. GRANT NUMBER

5c. PROGRAM ELEMENT NUMBER

6. AUTHOR(S)
Constantine G. Fountzoulas and Jerry C. LaSalvia

5d. PROJECT NUMBER

5e. TASK NUMBER

5f. WORK UNIT NUMBER

7. PERFORMING ORGANIZATION NAME(S) AND ADDRESS(ES)
U.S. Army Research Laboratory
ATTN: RDRL-WMM-B
Aberdeen Proving Ground, MD 21005-5069

8. PERFORMING ORGANIZATION REPORT NUMBER
ARL-TR-6623

9. SPONSORING/MONITORING AGENCY NAME(S) AND ADDRESS(ES)

10. SPONSOR/MONITOR'S ACRONYM(S)

11. SPONSOR/MONITOR'S REPORT NUMBER(S)

12. DISTRIBUTION/AVAILABILITY STATEMENT
Approved for public release; distribution is unlimited.

13. SUPPLEMENTARY NOTES

14. ABSTRACT
Advances in the numerical techniques and materials models have resulted not only in improved simulation tools for ballistic impact into single and multilayer armor configurations but also have contributed in the understanding of the physics involved. However, the ability of a numerical model to realistically predict the response of ceramic armor to ballistic impact depends mainly on the selection of appropriate material models and availability of appropriate data. In a presentation titled Ballistic Impact Damage in Hot-Pressed Boron Carbide, LaSalvia and coauthors experimentally studied the interaction of confined hot-pressed boron carbide (B_4C) targets impacted by laboratory-scale tungsten-based long-rod penetrators at velocities between 819 and 1205 m/s. An initial study of the ability of the existing material models to predict the observed damage induced by 93% tungsten heavy alloy (WHA) cylindrical projectiles striking confined cylinders of hot-pressed B_4C at velocities between 819 and 1205 m/s was performed. It was determined that the damage patterns were highly dependent on the properties of the confined ceramic and the impacting cylinder, whose failure behavior was difficult to model, and the strength and failure of material models used for the modeling. This report details the results of parametric studies conducted of various model parameters in an attempt to accurately simulate the ballistic response of confined hot-pressed B_4C targets.

15. SUBJECT TERMS
numerical analysis, ballistic, tungsten impactors, confined boron carbide, material models

16. SECURITY CLASSIFICATION OF:			17. LIMITATION OF ABSTRACT	18. NUMBER OF PAGES	19a. NAME OF RESPONSIBLE PERSON
a. REPORT	b. ABSTRACT	c. THIS PAGE			Constantine G. Fountzoulas
Unclassified	Unclassified	Unclassified	UU	20	19b. TELEPHONE NUMBER (*Include area code*) 410-306-0844

Standard Form 298 (Rev. 8/98)
Prescribed by ANSI Std. Z39.18

Contents

List of Figures

List of Tables

1. Introduction

Ceramics are materials that possess characteristics such as low density, high hardness, and high-compressive strength that make them ideal for use in light armor; however, ceramics are also brittle and have a low-tensile strength, which complicates the design of such systems. Numerous experimental investigations have been performed since the 1960s to develop an understanding of the behavior of ceramics under high-velocity impact, the phenomenology of ceramic failure, and the behavior of the failed ceramic under large pressures. These studies have been crucial in the development of ceramic material models (*1*).

The pioneering experimental and numerical work of Wilkins and coworkers gave a great deal of insight into the penetration process and failure phenomenology of ceramics used in composite armor (*2*). Their observations of ceramic failure were further expounded upon by the subsequent work of Shockey et al. (*3*) who performed a series of experiments with confined ceramic targets impacted by tungsten-nickel-iron rods at velocities from 0.8 to 1.4 km/s and from the recovered targets were able to detail the failure sequence in the ceramic. It was determined that if the projectile velocity is sufficient or if the ceramic is not adequately confined, the projectile loading begins to introduce tensile cracks near the impactor periphery. Ceramics possess low-tensile strength and when large tensile stress fields are introduced in the radial direction, they may form ring cracks, concentric around the impact point. Initially shallow, upon continued loading these ring cracks propagate in the direction of maximum principal tensile stress, typically on angles from 25° to 75° normal to the surface. They progress to the back surface of the ceramic and form large Hertzian cone cracks. As the loading increases further, the compressive strength beneath the penetrator is exceeded and microcracking begins. After the cone cracks form, the principal stresses redistribute to a circumferential direction, which result in tensile radial cracks forming like spokes on a hub from the impact site. Lateral cracks also form below the impact surface and intersect the radial and cone cracks forming fragments, which can break away from the impact site leaving a crater (*3*).

Although fractured and fragmented, the ceramic still resists penetration. If confined, the penetrator can only proceed by moving the ceramic out of the way. To do so, the projectile must pulverize it and force the pulverized material to flow laterally and then rearward (*1*). This zone of pulverized ceramic ahead of the projectile is known as the comminuted zone or the Mescall zone, after the work of Mescall and Weiss (*4*). Ceramic penetration resistance is a function of its compressive strength, hardness, pulverization, ceramic powder flow properties and abrasiveness, which serves to erode and consume the lead surface of the projectile (*3*).

Subsequent studies by Bless et al. (*5*) and Hauver et al. (*6*) also observed that if the ceramic is sufficiently confined, the projectile will flow laterally on the surface of the ceramic and not penetrate. These phenomena have become known as interface defeat or infinite dwell (*4*).

Recent x-ray experiments by Lundberg et al. (*7*) have been able to capture the transition from the projectile dwelling on the ceramic surface to penetration.

However, perhaps the most widely utilized and well known of the material models developed for ceramics are the ones developed by Johnson and Holmquist (*8*, *9*), which have become known as JH-1 and JH-2. Holmquist, et al. have also extended the ceramic model to account for phase transformation and this version is known as the JHB model (*10*). One significant difference between the models is that the JH-2 allows for a gradual degradation of the ceramic strength from the intact surface as the damage accumulates, while the ceramic strength in the JH-1 and JHB models does not degrade from the intact strength curve until the material is fully damage (D = 1.0).

This work investigates the ability of the existing ceramic material models to duplicate the damage of the confined boron carbide (B_4C) and further investigates the ability of the existing JH-2 ceramic material models to predict the observed damage, such as the lack of comminuted region, and short and long cracking introduced in confined cylinders of B_4C struck by a cylinder of tungsten carbide at high (819–1205 m/s) velocities (*9*). The effect of specific strength and failure model on the damage development is described and the contribution and sensitivity of these parameters on the accuracy of the solution when compared to the experimentally determined damage patterns are discussed.

2. Experimental Details

Details of the impact experiments have been reported by LaSalvia (*11*) and the experimental setup is shown in figure 1. The targets were center impacted at velocities ranging from 819 and 205 m/s. Following the cylinder impact experiments, photomicrographs were taken of the impacted surfaces. To preserve the impact surface integrity, the cylinders were impregnated with a cold mount epoxy and then extracted from their Ti-6Al-4V cups by carefully sectioning the cups (lengthwise) into several pieces. The final cross sections were 0.1–0.3 mm from the apparent center of impact and were subsequently examined by optical and scanning electron microscopy. A cross section showing the damage of the B_4C at impact velocity at 1205 m/s is shown in figure 2. The target was confined at the bottom of the Ti-6Al-4V “cup” (V = 0 m/s).

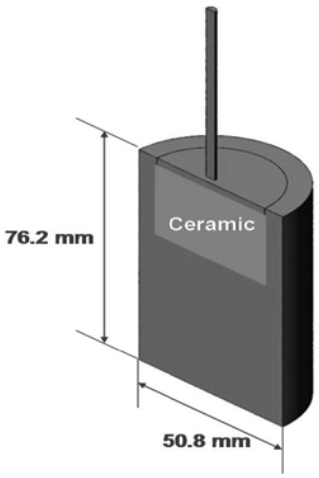

- PAD B4C (hot-pressed B_4C), BAE Advanced Ceramics
- 38.1-mm diameter by 38.1-mm-thick cylinders
- Ti6Al4V "cups" (50.8 × 76.2 mm)
- Slip-fit (< +/– 0.05 mm)
- 3.175-mm-thick Ti6Al4V cover (welded)
- 93% W alloy (WHA), L/D 20, 3.175 × 63.5 mm, 8.94 g (ρ = 17.9 g/cm^3, Y ≈ 1.4 GPa)
- Impact velocity 819, 1052, 1063, 1198 and 1205 m/s

ρ (g/cm^3)	Grain Size (μm)	E, ν (GPa)	HK4 (GPa)	K_{IC} (MPa*m$^{1/2}$)	σ_b (MPa)	Phases
2.52	15	450, 0.17	18.9	2.9	400	B4C, C

Figure 1. Target configuration and B_4C measured properties.

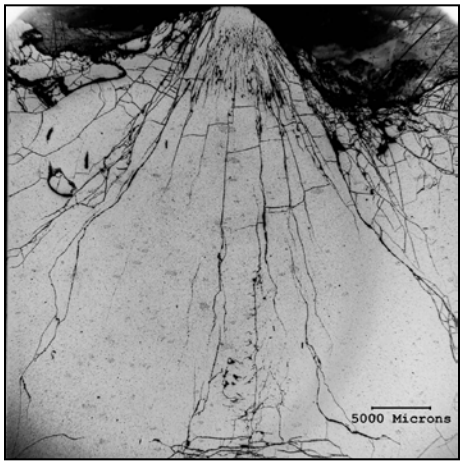

Figure 2. SEM photomicrograph of B_4C failure pattern at 1205-m/s impact velocity.

3. Numerical Simulations

The ballistic behavior of all the targets (figure 1) was studied with three-dimensional (3-D) models and simulated using the nonlinear ANSYS/AUTODYN commercial package (*12*). The material models used were obtained from the AUTODYN library (*12*). All materials were discretized using smooth particle hydrodynamic (SPH) solver with a particle size of 0.25 mm. The Ti-6Al-4V sleeve and cover were modeled using a Puff equation of state (EOS), Von Mises strength, and a Grady spall failure model taken from the AUTODYN Material Library. The

tungsten heavy alloy (WHA) projectile was modeled using a shock EOS, and a Johnson-Cook strength model (*3*). The B_4C was modeled using a polynomial EOS, JH-2 strength and failure models. In addition, the tensile failure criterion for the B_4C was set to either the hydro tensile or minimum pressure, or principal stress with or without crack softening. In the effort to capture the damage of the B_4C, various criteria were used.

4. Initial Numerical Study

As a first attempt, all materials were modeled using their corresponding material EOS, strength and failure models as they appear at the AUTODYN library without any modification. In particular, the tensile failure of the JH-2 failure material model of B_4C was set to hydro tensile (P_{min}). The results for all simulations did not correlate well with the experimental observations. According to LaSalvia (*11*) the B_4C for all impact velocities, 819, 1052, 1063, 1198, and 1205 m/s was cracked and the projectile was fractured (figure 3). While the simulated extent of damage induced to the B_4C as shown in figure 3 resembles qualitatively the extent of damage shown on the x-ray radiographs, little cracking of the B_4C appears only at 1205-m/s impact velocity after 40 μs. Subsequent studies were performed by utilizing changing the tensile failure of the JH-2 failure model of the B_4C to principal stress without crack softening, and crack softening with stochastic failure with stochastic variance $\gamma = 16$. The resulting simulation predictions of damage induced in the B_4C also did not correlate well with the experimental observations beyond 30 μs of simulation time. Figures 3 and 4 show the damage evolution of the target for the cases of principal stress criterion without crack softening, and with crack softening with stochastic variance at impact velocities 819 and 1205 m/s, respectively. Simulations for times beyond 40 μs for impact velocity of 819 m/s and 25 μs for impact velocity of 1205 m/s showed complete B_4C cracking. The conclusions of the initial study are summarized as follows and in figures 3 and 4:

- The hydro-tensile failure criterion was not able to introduce cracking in the B_4C target even when it was decreased from 7300 to 2000 MPa.
- The principal stress failure model with crack softening and stochastic variance of the B_4C replicated partially the ceramic failure for all cases studied for two-dimensional (2-D) and 3-D simulations.
- For planar symmetry for the (2-D) simulation the cracking was replicated well up to 35 μs.
- When using the principal stress failure model with crack softening only, the ceramic crack is excessive for both, low- and high-impact velocity.
- For (2-D) axisymmetric simulation, the cracking was replicated well up to 35 μs.

- The (2-D) axisymmetric modeling introduces an artificial target failure along the axis of symmetry. For the 3-D modeling the target failure was replicated poorly up to 40 μs.
- No B_4C failure model managed to stop the projectile from penetrating the target while replicating the introduced cracking satisfactorily.
- The target penetration resulted in bulging of the Ti-6Al-4V "cup," which was not observed experimentally.

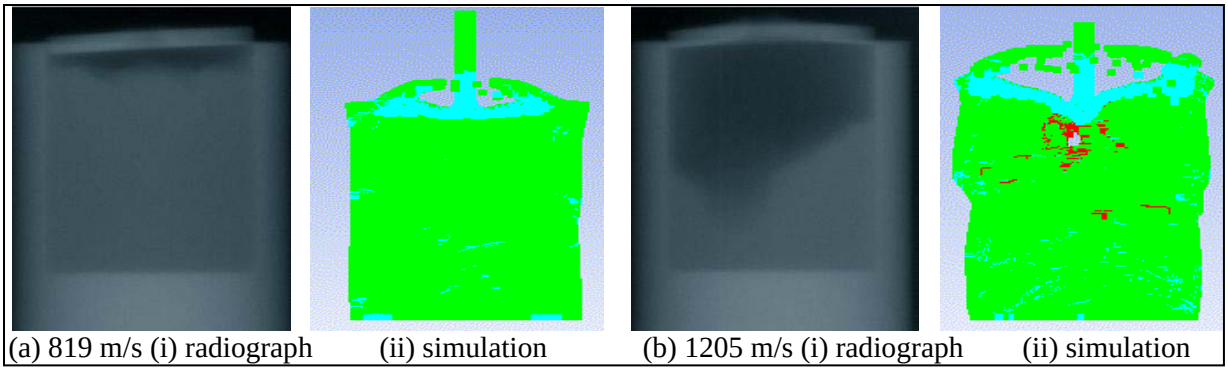

Figure 3. Static x-ray radiographs of B_4C and simulated damaged status (40 μs) using hydro-tensile failure model.

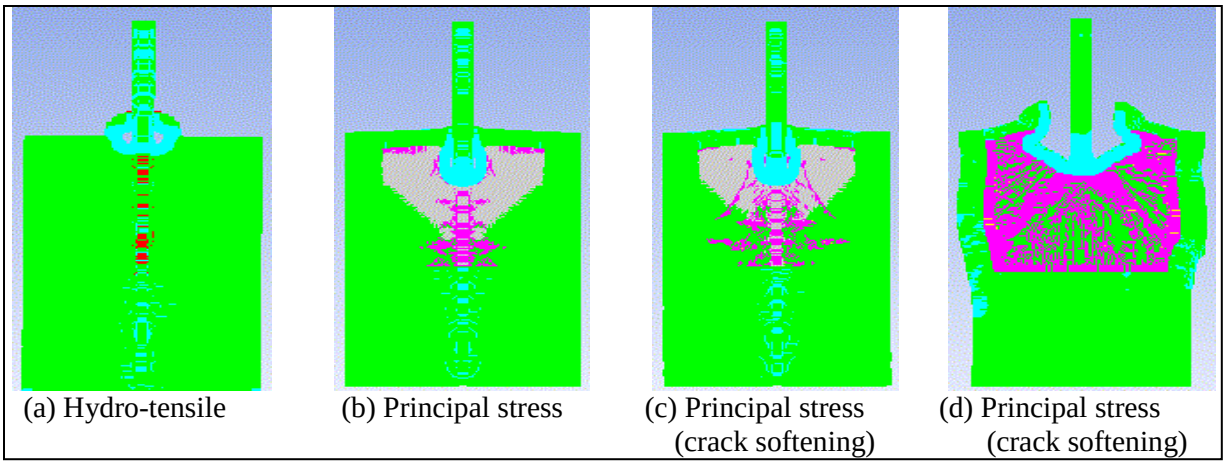

Figure 4. Simulated damage status after 25 μs at 1205 m/s impact velocity: a–c, 2-D axisymmetric; and d, planar symmetry.

5. Material Models Parameter Modifications

To improve the predictive capabilities of the existing material models educated trial and error modifications of shear modulus, bulk modulus and hydro-tensile limit of the AUTODYN library values were conducted. Table 1 shows the modifications of shear modulus, bulk modulus and hydro-tensile limit of the AUTODYN library values, which reproduced most successfully the

failure pattern of the B_4C and WHA projectile. Figure 5 shows the simulated failure pattern of the encapsulated B_4C at 1205 m/s impact velocity obtained with unmodified AUTODYN library strength and failure models. Although the projectile was stopped the simulated failure pattern of the ceramic is poor compared to the experimental results. Figures 6–10 show the simulation results obtained with the modified material models. For impact velocities 1052, 1063, 1198 and 1205 m/s the simulations duplicated successfully the extent of damage under the cover plate (figures 6–9). However, for impact velocity 819 m/s the damage extent under the cover was smaller than observed experimentally (figure 10). The projectile was stopped for all impact velocities. Although the overall simulated damage appears to be like a mirror image of the actual one, the extent of the simulated damage is remarkably similar (figures 6 and 7). The simulated damage extent at 1063 m/s appears larger and similar to the simulated damage higher observed at 1205 and 1198 m/s (figures 6 and 7). The simulated damage at impact velocity 1052 m/s was almost identical to the experimental damage.

However, the duplication of the only experimental existing detailed cracking pattern at 1205 m/s (figure 2) is very poor (figure 6).

Table 1. Most successful material models parameter modifications.

Parameter	**AUTODYN Library**	**Modifications (Most Successful)**
G (Shear Modulus) [***Strength***] (GPa)	199	100
K (Bulk Modulus) [***EOS***] (GPa)	230	117
HTL (Hydro-Tensile Limit) [***Failure***] (GPa)	–1.9	–1.0

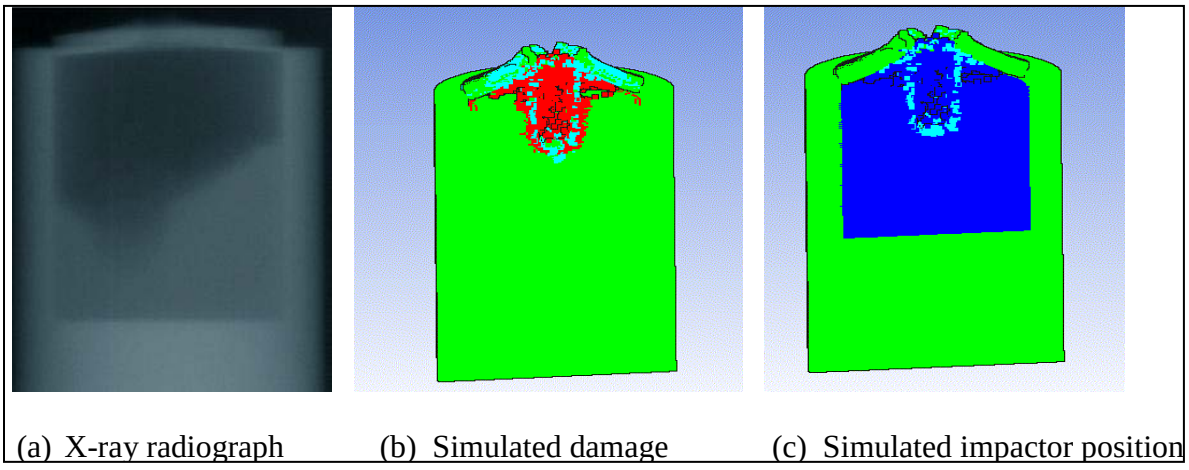

(a) X-ray radiograph (b) Simulated damage (c) Simulated impactor position

Figure 5. Simulation using AUTODYN library parameters: impact velocity 1205 m/s.

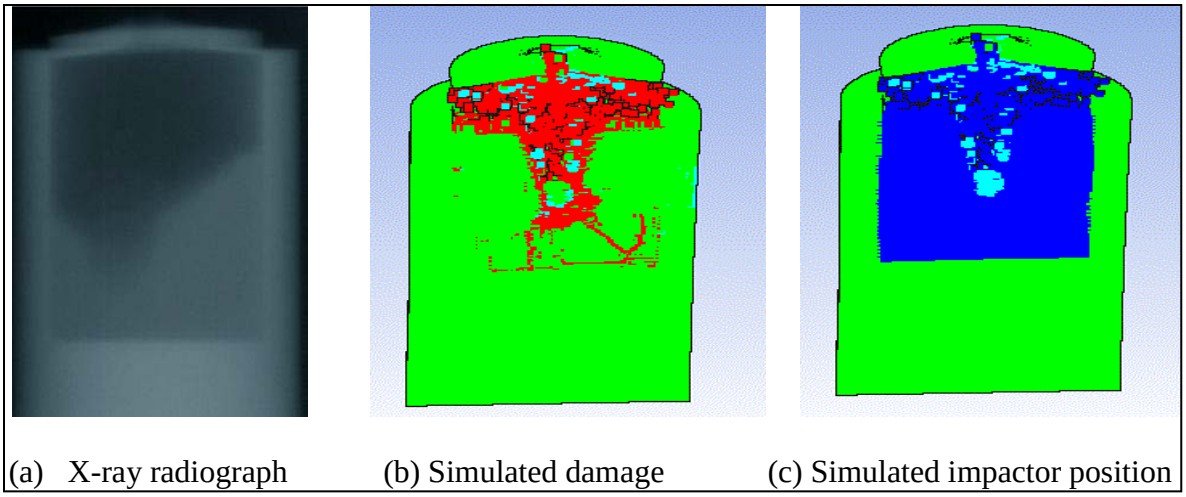

Figure 6. Simulation using modified parameters: impact velocity 1205 m/s.

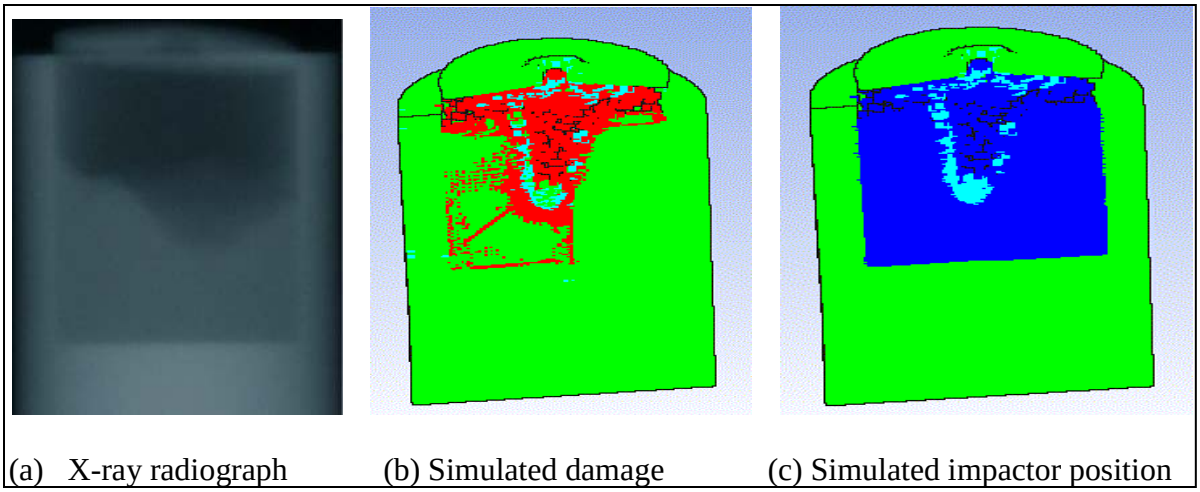

Figure 7. Simulation using modified parameters: impact velocity 1198 m/s.

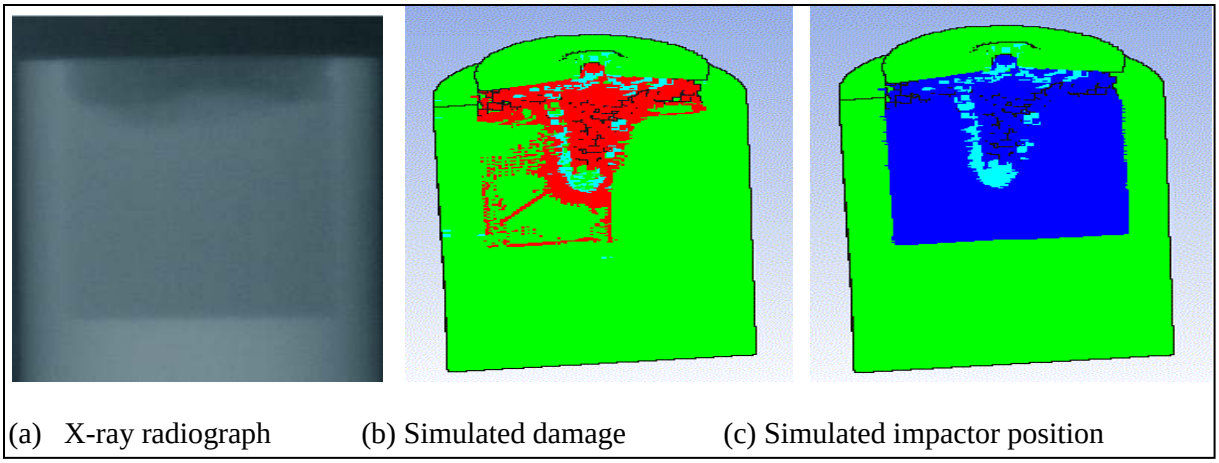

Figure 8. Simulation using modified parameters: impact velocity 1063 m/s.

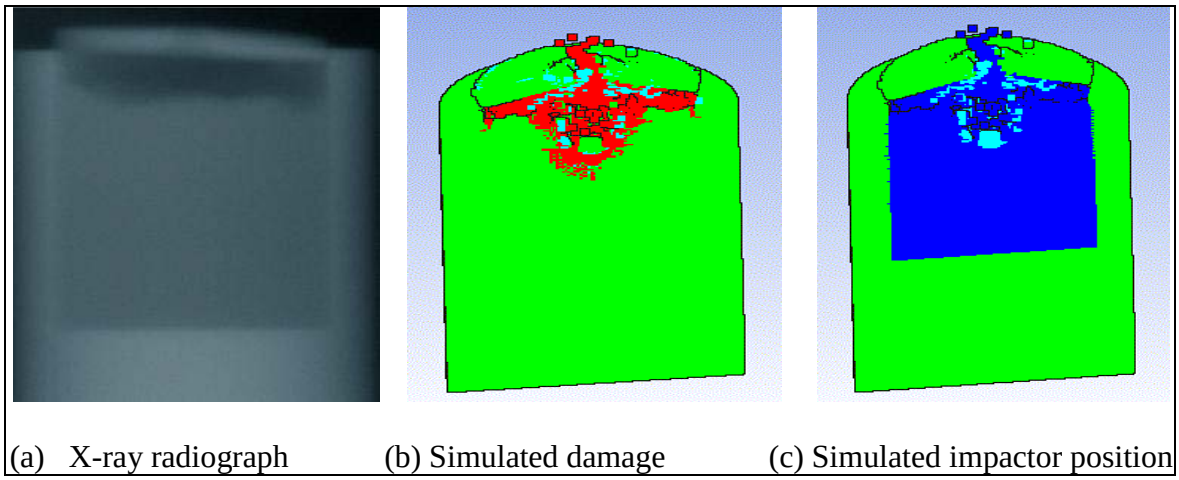

(a) X-ray radiograph (b) Simulated damage (c) Simulated impactor position

Figure 9. Simulation using modified parameters: impact velocity 1052 m/s.

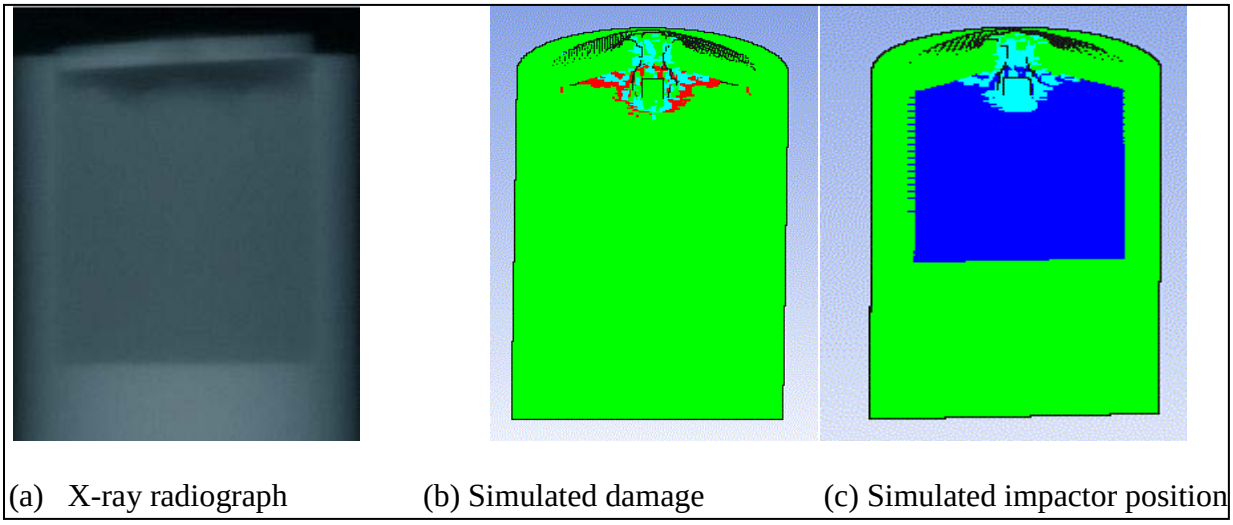

(a) X-ray radiograph (b) Simulated damage (c) Simulated impactor position

Figure 10. Simulation using modified parameters: impact velocity 819 m/s.

6. Discussion

The modifications of the shear modulus, bulk modulus, and hydro-tensile limit successfully duplicated the extent of the damage under the cover plate at impact velocities 1052, 1198, and 1205 m/s. Although the simulation at 1063 and 819 m/s produced larger and smaller damage extent under the cover, respectively, the simulated damage was comparable to the experimental damage. The projectile was stopped for all impact velocities and the cover plate was broken—in agreement with the experimental results.

As it is shown in table 1, to successfully reproduce the failure pattern of the B_4C, we had to reduce the shear and bulk modulus, and the hydro tensile to about 50% of the AUTODYN library corresponding values. This may be partially attributed to the smaller values of these properties of the B_4C due to its recently experimentally observed amorphization (*13, 14*).

The failure of the existing strength and failure material models of all the parts of the target architecture to capture the experimentally observed cracking pattern of the ceramic and the failure of the projectile may also be attributed to the inability of these models to account for the continuously developing compressive stresses caused by the ceramic confinement during the impact.

The simulations provide a significant amount of insight into the problem and could provide another measure that could be quantified through experiments. The simulations also showed that the higher the target cracking the more the retardation of the penetration process. The authors believe that due to the ceramic confinement, the strength of the failed ceramic is higher than that predicted by the B_4C existing failure model, thus resulting in more effective defeat of the impacting WHA cylindrical impactor.

7. Conclusions

The Johnson-Holmquist series of ceramic material models have been developed for the high-velocity impact and penetration of ceramics; their applicability to the confined hot-pressed B_4C target hit by cylindrical WHA impactor is of interest. The ability of the phenomenological Johnson-Holmquist ceramic model to predict the observed damage patterns induced by the WHA impactor striking confined cylinders of hot-pressed B_4C at velocities from 819 to 1205 m/s was investigated. The simulation results of this investigation using modified shear and bulk modulus and hydro-tensile limit can be summarized as follows:

- JH-2 model with standard properties did not reproduce the damage of the confined B_4C to any satisfactory level.
- JH-2 model with modified material models reproduced the overall B_4C damage from 1052 to 1204 m/s impact velocity rather accurately when compared to the x-ray radiographs.
    - However, the overall reproduction for 819 m/s impact velocity was not as good as the rest of them.
    - The 1198 and 1205 m/s simulations also reproduced the asymmetrical damage as shown in the radiographs.

- High-impact velocity simulation failed to reproduce accurately the experimental cracking pattern of the B_4C.
- The projectiles were stopped for all impact velocities.

The efforts to duplicate the cracking pattern of the B_4C by modifying further the existing JH-2 material models continue for more accurate prediction of the failure pattern. Moreover, efforts are anticipated to be improved by any measurement of the properties of the amorphous phase of the B_4C.

8. References

1. Fountzoulas, C. G.; Normandia, M. J.; LaSalvia, J. C.; Cheeseman, B. A. Numerical Simulation of the Cracking of Silicon Carbide Tiles Impacted by Tungsten Carbide Spheres *22nd IBS*, **2005**, Vancouver, Canada.
2. Wilkins M. L.; Cline C. F.; Hondol, C. A. Tech .Rep. UCRL-50694; Lawrence Rad. Lab. 1969.
3. Shockey, D. A.; Marchand, A. H.; Skaggs, S. R.; Cort, G. E.; Burkett, M. W.; Parker, M. W. Failure Phenomenology of Confined Ceramic Targets and Impacting Rods. *Int. J. Imp. Eng.* **1990**, *9* (3), 263–275.
4. Mescall, J., Weiss V. Materials Behavior Under High Stress and Ultrahigh Loading Rates. *Part II. Proceeding of the 29th Sagamore Army Conference, Army Materials and Mechanics Research Center:* Watertown, MA, 1984.
5. Bless S. J.; Brar, N. S.; Kanel, G.; Rosenberg, Z. Failure Waves in Glass. *J. Am. Cer. Soc.* April **1992,** *75* (4), 1002–1004.
6. Hauver, G. E.; Netherwood, P. H.; Benck, R. F.; Kecskes, L. J. Enhanced Ballistic Performance of Ceramic Targets. *19th. Army Science Conference*, 1994.
7. Lundberg P.; Renström R.; Holmberg, L. An Experimental Investigation of Interface Defeat at Extended Interaction Times. *Proc. 19th. Int. Symp. Ballistics*, 2001; Vol. 3, pp 1463–1469.
8. Johnson G. R.; Holmquist, T. J. A Computational Constitutive Model for Brittle Materials Subjected to Large Strains, High Strain Rates and High Pressure. *Proc. EXPLOMET Conference*, San Diego, CA, 1990.
9. Johnson, G. R.; Holmquist, T. J. *An Improved Computational Constitutive Model for Brittle Materials*. In Proceedings of the APS Conference on High-Pressure Science and Technology; Schmidt, S. C.; J. Shaner, W.; Samara, G. A.; Ross, M. (eds.), Colorado Springs, CO, June 1993, pp 981–984.
10. Holmquist, T. J.; Johnson, G. R.; Beissel, S. R. *J. Applied Physics* **2003**, *94*.
11. LaSalvia, J. C. Ballistic Impact Damage in Hot-Pressed Boron Carbide. *34 ICACC*, Daytona Beach, FL, 25–29 January 2010.
12. ANSYS/AUTODYN Vol. 12.1, Manual, Century Dynamics Inc., Concord, CA.

13. Daphalapurkar, N. G.; Hu, K. T.; Ramesh, J. Specimen Size Effects on the Dynamic Failure Strength of Brittle Materials. *Presentation, 36 ICACC*, Daytona Beach, FL, 22–27 January 2012.

14. LaSalvia, J. C.; Shanholtz, E. R. U.S. Army Research Laboratory. Further Results on Nanocrystallization Features in Ballistically-Impacted Boron Carbide. *Presentation, 36 ICACC*, Daytona Beach, FL, 22–27 January 2012.

NO. OF COPIES	ORGANIZATION
1 (PDF)	DEFENSE TECHNICAL INFORMATION CTR DTIC OCA
1 (PDF)	DIRECTOR US ARMY RESEARCH LAB IMAL HRA
1 (PDF)	DIRECTOR US ARMY RESEARCH LAB RDRL CIO LL
1 (PDF)	GOVT PRINTG OFC A MALHOTRA
1 (PDF)	UNIV OF FLORIDA G SUBHASH
1 (PDF)	USARL SOLID MECHANICS MECH SCI DIV PROGRAM MANAGER L C RUSSELL
2 (PDF)	NSF S MCKNIGHT G PAULINO
1 (PDF)	DARPA M MAHER
1 (PDF)	US ARMY ARDEC AMARD AAR AEE W E BAKER
1 (PDF)	COMMANDER US ARMY RSRCH OFC RDRL ROE M D STEPP
3 (PDF)	JOHNS HOPKINS UNIV DEPT OF MECH ENGRE & CIVIL ENGRG S GHOSH L GRAHM-BRADY K T RAMESH

ABERDEEN PROVING GROUND

NO. OF COPIES	ORGANIZATION
44 (PDF)	DIR USARL RDRL CIH S J CAZAMIAS
	RDRL WM P BAKER S KARNA P PLOSTINS
	RDRL WML M ZOLTOSKI
	RDRL WML A W OBERLE
	RDRL WML B B RICE R PESCE-RODRIGUEZ
	RDRLWML G W DRYSDALE
	RDRL WML H J NEWILL B SCHUSTER
	RDRL WMM J BEATTY R DOWDING J ZABINSKI
	RDRL WMM A J SANDS J TZENG E WETZEL
	RDRL WMM B T BOGETTI R CARTER B CHEESEMAN C FOUNTZOULAS G GAZONAS D HOPKINS T JENKINS R KARKKAINEN B LOVE P MOY B POWERS C RANDOW T SANO R WILDMAN C YEN
	RDRL WMM C J LA SCALA
	RDRL WMM D E CHIN K CHO

NO. OF
COPIES ORGANIZATION

RDRLWMM E
J ADAMS
M BRATCHER
M COLE
J LASALVIA
P PATEL
J P SINGH
RDRL WMM F
L KECSKES
H MAUPIN
E KLIER